An Integral Design of Ground Power Unit Supply for Aircraft Applications

Marco Rivera
Faculty of Engineering
University of Talca
Curico, Chile
marcoriv@utalca.cl

Daniel Faundez
Faculty of Engineering
University of Talca
Curico, Chile
dfaundez12@alumnos.utalca.cl

Johann Kolar
Power Electronic Systems Laboratory
ETH Zurich
Zurich, Switzerland
kolar@lem.ee.ethz.ch

Patrick Wheeler
Dept. of Electrical & Electronic Engineering
The University of Nottingham
Nottingham, UK
Pat.Wheeler@nottingham.ac.uk

Jose A. Riveros
Faculty of Engineering
University of Talca
Curico, Chile
jriveros@utalca.cl

Sergio Toledo
Faculty of Engineering
University of Talca
Curico, Chile
stoledo@utalca.cl

***Abstract*—A new ground power unit configuration is introduced in this paper. The architecture comprises a six-pulse rectifier with active current injection in the input stage to achieve high-performance conversion with low polluted ac spectrum, whereas the output voltage is synthesised with a neutral-point clamped inverter to attain an output with high quality that simplifies the LC filter development. The entire design of the static power converter is presented in this work, while simulation results are conducted for the validation of this proposal. A regulated output voltage with low distortion accomplishing the standards confirms the viability of this scheme.**

***Index Terms*—Ground power unit, ac-dc power converters, neutral-point clamped inverter**

I. Introduction

Modern developments in the aerospace industry increase the use of motor drives and power electronics replacing the mechanicals actuators and following the emerging concept of more-electric aircraft [1]. Additionally, the agreements of the green agenda force restrictions to reduce both consumption of fossil oil and noise pollution. These constrains also ought to be obeyed during the refuelling and loading of the aircraft. Consequently, an external power source with high-performance is required to supply electricity to the plane during these operations complying with the standards of this application [2, 3]. The solution relies on static power conversion techniques and it is known as ground power unit (GPU) [4]. This proposal is used for civil and military purposes [5, 6], providing constant ac output voltage (magnitude and frequency) regardless of the load and isolated from the ac mains [7].

The GPU must convert the mains voltage to a three-phase system with 115 Vrms at 400 Hz. The classical architecture comprises an input filter, a rectifier, an inverter, an output filter, and an isolation transformer. Alternatively, matrix converters have been considered for this application [4, 5]. The input filter is linked to the rectifier in order to minimise the impact of the ac-dc conversion. Multi-pulse, two-level and multilevel rectifiers have been proposed in the ac-dc stage in order to minimise the ac current harmonics [8]. The multilevel technology has been proposed recently for the dc-ac stage [9]. These power converters are suitable for this use taking into account the higher quality output, lower common-mode voltage, and lower dv/dt emissions with respect to the conventional two-level inverters [10]. The ac output is commonly linked to an LC filter to mitigate the current ripple and the aircraft has to be isolated from the static converter by using a galvanic transformer. Finally, for the control of this configuration different schemes such as linear proportional-integral, proportional-resonant, dead-beat, selective harmonic mitigation, sliding mode were proposed [11-15].

The employment of diode bridge rectifiers with passive filters is straightforward at the sake of not providing the best performance in the ac-dc stage of the GPU. This combination might affect the operation (causes distortion), uses bulky passive components and requires complex design for high-order implementations [16]. Current injection methods are more attractive and suitable for the characteristics of this application, providing high-performance and small size/weight configurations [17, 18]. This proposal designs the GPU using an active third harmonic injector [19]. This provides low switching frequency, simple control and has the capability of generating sinusoidal current in the mains side.

Multilevel inverters were recently proposed for GPU [20]. This technology is appropriate considering the requirements of this application such as the low frequency index (ratio between the sampling and the fundamental frequencies) due to the demanded output frequency (400 Hz, eight times the conventional value) that constraints the quality of the output for conventional voltage source converters. The model introduced includes a three-level neutral-point clamped (NPC) inverter, which is one of the most promoted topologies for medium- and high-power purposes [10]. Modulation and control strategies for this inverter have been extensively studied and can be implemented for this development.

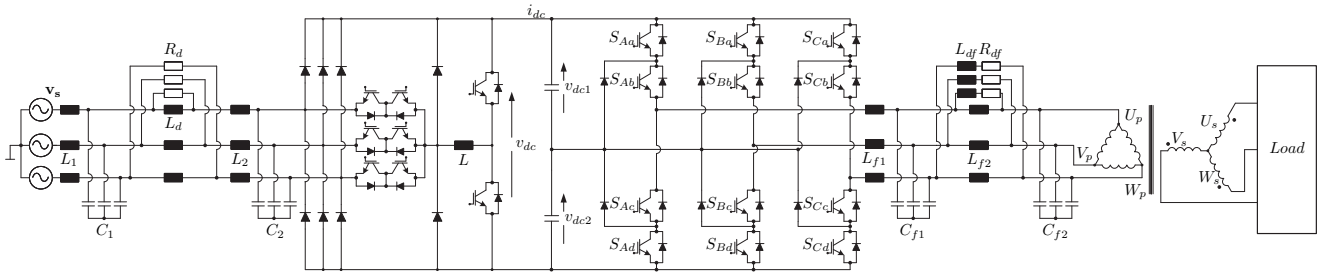

Fig. 1. Scheme of the developed ground power unit for aircraft applications.

The paper is organised as follows. First, the design of the GPU is described including the filter and control strategies for the power conversion in Section II. Then, Section III presents the simulation tests and assesses the results. Finally, the conclusions are summarised in the last section of this manuscript.

II. Development of the New Ground Power Unit Topology

The introduced GPU configuration is presented in Fig. 1. The ac-dc conversion stage is a three-phase six-pulse diode bridge rectifier with an active third harmonic injection filter. This supplies the dc-link of a three-level NPC inverter that generates an ac of 115 Vrms at 400 Hz output for the aircraft. The GPU is linked to the latter through an isolation transformer accomplishing the standard.

The high-efficiency rectifier with active current injection has been introduced in [21]. The injection circuit uses three bidirectional power switches, while the current shaping employs a half-bridge inverter and an inductor. The current injection method is simple reporting a low switching frequency. At every time, only the bidirectional switch connected to the phase with the lowest absolute voltage value is turned on with a small overlap to avoid over-voltage in the inductor. Nevertheless, Two diodes have been included next to the inductance for safety. The half-bridge inverter is modulated to generate the third harmonic current synchronised with the mains. The dc voltage is determined by the ac power source.

The NPC inverter is controlled by means of a pulse width modulation (PWM) technique that balances the dc capacitors by using the method proposed in [22]. This is for the sake of simplicity in a preliminary validation of the developed design.

TABLE I
Switching control for the current injection circuit

Sector	S_a	S_b	S_c
0°-60°	0	1	0
60°-120°	1	0	0
120°-180°	0	0	1
180°-240°	0	1	0
240°-300°	1	0	0
300°-360°	0	1	0

The design procedure of the entire GPU scheme, including the passive filters, are detailed as follows.

A. Current Modulation and Third Harmonic Injection

The current injection control is simple and follows the technique implemented in [19]. Then, the bidirectional power switch activation is synchronised with the mains as is summarised in Table I. Notice that the switching frequency is only two times the fundamental component of the ac power source and the injection is performed in the phase with the lowest voltage, achieving an positive impact in the losses and the power required by this circuit. The controller only needs comparators to generate the switching signals of the bidirectional power switches.

The half-bridge inverter controls the current injected through the bidirectional power switches. The reference current is a semi-triangular waveform synchronised with the ac mains but at six times the fundamental component frequency. The current regulator is a proportional-integral controller plus PWM to generate the switching signals of the half-bridge inverter and to synthesise the reference in the inductor (i_L).

This active current injection scheme generates a sinusoidal waveform in the ac line with a quasi unitary power factor. However, with this additional circuitry the output voltage cannot be controlled and its value depends on the magnitude of the ac mains.

B. Inductor

For the design of the inductance L, the ac voltage, switching frequency (f_s) and semi-triangular peak-to-peak current value (Δi) should be considered. The value of the inductance is related to these parameters, as follows:

$$L \leq \frac{\sqrt{3} \times v_{a,rms}}{2 \times f_s \times \Delta i} \tag{1}$$

being $v_{a,rms}$ the rms phase voltage of the mains. Considering $\Delta i = 25\%$ of the maximum current ($I_{L,max} = P/V_N$), the rated power $P = 10$[kW], $V_N = 480$[V] and the switching frequency $f_s = 36$[kHz]; the ripple current $\Delta i = 2.6$[A] and the inductance L yields

$$L \leq \frac{\sqrt{3} \times 480}{4 \times 36000 \times 2.6} \leq 2.2[mH] \tag{2}$$

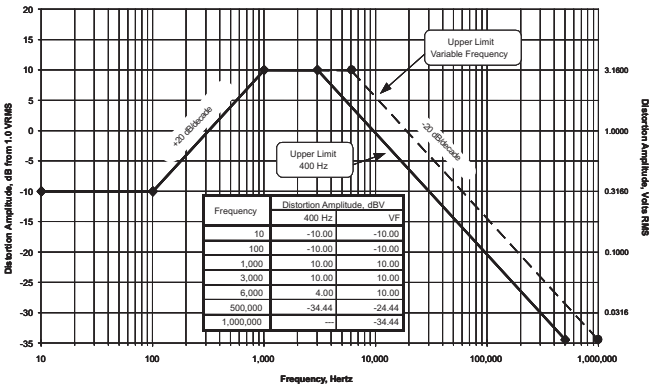

Fig. 2. Spectrum of 400[Hz] defined by the standards.

C. Capacitors

The capacity of the dc-link, C, is designed considering the voltage ripple of the diode bridge output. This commonly is calculated as follows

$$C \ \leq \ \frac{I_N}{2 \times \Delta v \times f_s}(1 - m_{min}), \tag{3}$$

with m_{min} being the minimal modulation index, while Δv is the voltage ripple. For this proposal, the maximum voltage ripple $\Delta v \ = \ 1.5\%$ of the diode bridge output voltage. Then, the series equivalent capacitor is:

$$C \ \leq \ \frac{2.6}{2 \times (0.015 \times \sqrt{3} \times 480) \times f_s}(1 - 0.5) \ \leq \ 12[\mu F] \tag{4}$$

Next, by assuming that C_1=C_2, the series capacitors are:

$$C_1 = C_2 = 24[\mu F] \tag{5}$$

D. Control of the NPC Inverter

The dc-ac stage is a three-level NPC power converter linked to the aircraft through a Δ-Y transformer. In order to provide simplicity in the introduction of this proposal, the inverter is controlled by using a PWM algorithm that balances the neutral-point of the dc-link. The variation of the dc-bus voltage due to the voltage ripple of the bridge rectifier is included in the modulation strategy by using a measurement of the dc-link voltage. The minimization of the mid-point current of the dc-bus is performed via the PWM method by injecting zero-sequence in the reference voltage. The injected amount is proportional to the difference between the capacitors' voltages [22]. Thus, the drift of the capacitors' voltages is regulated within a small band.

E. Output Filter

The output filter must comply to the quality standards of the output voltage for aircrafts. The following requirements rule this application and are summarised in the frequency response of Fig. 2:

- Peak-to-peak output voltage ripple Δv_{out} bellow 1.0% respect to the nominal value [3]. Then, $\Delta v_{out} \leq 4.6$[V].
- Peak-to-peak filter inductor current ripple Δi_L bellow 30% of the nominal output current peak value. Particularly, $\Delta i_L \leq 6.4$[A].
- Maximum small signal output impedance Z_{out_max}. This parameter is set to 3.5 times the maximum output impedance, $Z_{out\_max} \leq 3.5[\Omega]$.
- Meet the standard according to [3] for conducted emission levels.
- Additionally, the output filter should have minimum weight, minimum value, minimal cost and/or minimal losses.

These requirements are the constraints in the design process of the output filter. Additionally, electric restrictions such as maximum reactive filter capacitor current ought to be considered. Proceeding according to the guidelines for optimum parameters of [23], the LC bank of the filter is identified and it is possible to evaluate single- or multi-stage topologies for this application. The analysis of [23] demonstrates that single-stage filter does not comply with the previous criteria and the EMI stipulations at the same time. Let us consider the following alternatives to overcome these limitations:

1) Interleaved bridge-leg per phase linked in parallel to a single-stage filter.
2) Larger number of voltage levels to decrease the high frequency output voltage ripple.
3) Diversified bridge-legs per phase can be linked and operated in parallel with a single stage filter.
4) Larger number of stages to attain higher attenuation for higher frequency components (>150[kHz]).

The last option enables a reduction of the size and cost. The optimum design is achieved with a two-stage LC bank. Let us consider n and k as the scaling weights of the second stage designed with the aim of reducing the total volume. Following the procedure of [23] sustained by commercial information, the smaller filter is $V_{f,min}$ =209.2cm^3 and it is obtained for $n \ = \ 0.01$ and $k \ = \ 0.9$. A parallel R_d-L_d damping branch ($L_d \ = n L_f/2$) is added for safety purposes under possible resonance sources, see Fig. 1.

The maximum voltage ripple is given by the following expression:

$$\Delta v_{out} \ = \ \frac{m(1-m)v_{dc}}{16 L_f C_f f_s^2} \ \leq \ 4.6[V] \tag{6}$$

where m is the modulation index and f_s is the switching frequency (f_s =36[kHz]). Notice that Δv_{out} is proportional to the dc-link voltage v_{dc} and inversely proportional to f_s.

The current ripple in the inductance is given by:

$$\Delta i_L \ = \ \frac{m(1-m)v_{dc}}{2 L_f f_s} \ \leq \ 6.4[A] \tag{7}$$

Notice that Δi_L is independent from C_f, and it is defined by the dc-link voltage and the switching frequency.

The output impedance can be attained as follows ($Z_{in} = v_{dc}/(2\Delta i_{out})$):

$$Z_{out} \ = \ \frac{L_f}{2(1-m) C_f Z_{in}} \ \leq \ 3.5[\Omega] \tag{8}$$

The output impedance depends on the ratio L_f/C_f. The emissions are also considered following the response of Fig. 2, and the standard [3] with maximum distortion [24].

The peak reactive current in the capacitor is expressed as:

$$i_{c,max} \;=\; w_o C_f \sqrt{2} v_{out,n} \;\leq\; 3[A] \tag{9}$$

where $w_o = 2\pi 400$. Finally, the parameters are obtained for the different design criteria considering a switching frequency of $f_s = 36$[kHz]:

- L_{f1} =574[μH]
- C_{f1} =3.58[μF]
- L_{f2} =5.74[μH]
- C_{f2} =3.22[μf]
- L_d =2.87[μH]

The damping resistance R_d is calculated following the procedure of [25], where the peak output impedance reduction is attained for a given L_d. The result is shown as follows:

$$\begin{aligned} R_d &= R_o Q_{opt} \\ R_o &= \sqrt{L_{f2}/C_{f2}} \\ Q_{opt} &= \sqrt{\frac{r(3+4r)(1+2r)}{2(1+4r)}} \end{aligned} \tag{10}$$

where $r = L_d/L_{f1}$. Thus, $R_d \;=\; 1.21\Omega$.

F. Isolation Transformer

The GPU is connected to the aircraft through a delta-star isolation transformer. This configuration mitigates the effect of load imbalances and distortions. The primary-to-secondary turn ratio is designed as follows:

$$\begin{aligned} \frac{N_p}{N_s} &= a \\ V_s &= \frac{\sqrt{3} v_o}{a} \end{aligned} \tag{11}$$

III. Results

The GPU is implemented in a Gecko Simulation environment to demonstrate the viability of this design. First, the input filter and the active current injector are removed from the developed GPU to present the natural response of the system without these stages. Next, the ac current characteristics when only third harmonic current is injected by active network is analysed. In the third assessment, the entire developed topology performance is presented.

The response of the GPU when only the three-phase diode rectifier is implemented in the ac-dc stage is indicated in Fig. 3. The mains' voltage and current (both for phase a) along with the dc-voltage distributed in the capacitors are shown. The resulting ac current, Fig. 3b, is the well-known six-pulse pattern with significantly high distortion, which is unacceptable for this application. On the other hand, the modulation technique implemented in the NPC inverter demonstrates acceptable performance balancing the capacitor's voltages with imperceptible differences, while in the aircraft side sinusoidal behaviour is accomplished ensuring 115[V] at 400[Hz] as indicated in Fig. 4.

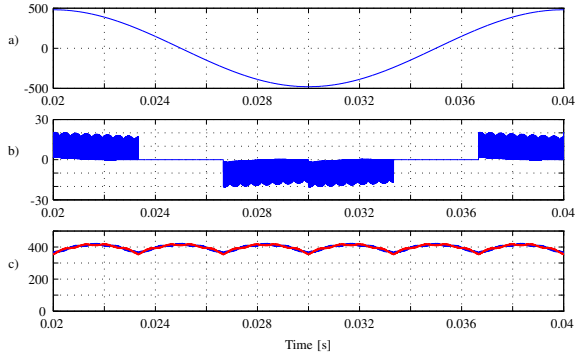

Fig. 3. Performance of the GPU in the dc-side without the input filter and the injection circuit: a) power source voltage v_{sA}[V]; b) ac line current i_{sA}[A]; c) capacitor voltages v_{dc1}[V] (red line), v_{dc2}[V] (blue line).

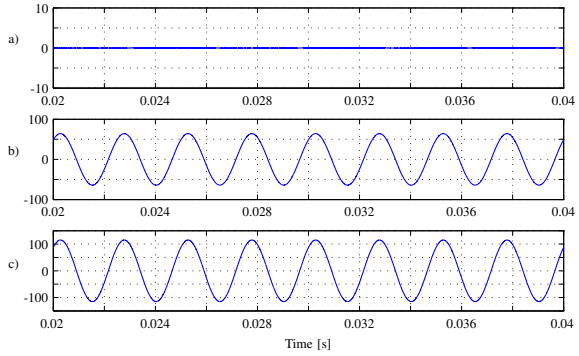

Fig. 4. Performance of the GPU in the output ac-side without input filter and injection circuit: a) IAF current i_L[A]; b) load current i_u[A]; c) load voltage v_u[V].

The second test is conducted by adding the third harmonic injection scheme. The active network enhances the quality of the currents in the mains side with respect to the previous case, and is synchronised with respect to the phase voltage (high power factor) as depict figures 5a and b. However, this is still highly distorted and does not meet the requirements of these applications. The balance of the capacitor voltages v_{dc1} and v_{dc2} again are kept within a very small band by using the modulation algorithm, see Fig. 5c. The semi-triangular current injected by the active circuitry is presented in Fig. 6a, while figures 6b and 6c show the response in the aircraft side. The output voltage is regulated properly with sinusoidal waveform and the voltage and frequency specified by the standard [3].

Finally, simulations of the entire design are carried out. Thus, the input filter together with the active third harmonic current technique are shaping the ac current at the input, while the NPC inverter regulates the output with the PWM method to supply the load demand. The behaviour of the variables of the mains side is drawn in Fig. 7. The resulting ac currents (Fig. 7b) present low harmonic content with high power factor, whereas the admissible performance in the dc-link is maintained as indicated in Fig. 7c. The active current

injection along with the ac output characteristics observed in Fig. 8 are the same as the previous two tests.

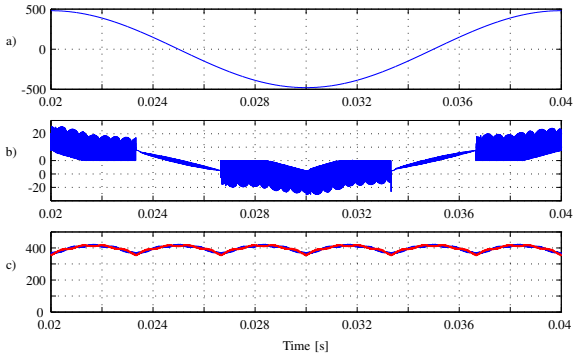

Fig. 5. GPU performance with the active current injection: a) source voltage v_{sA}[V]; b) source current i_{sA}[A]; c) capacitor voltages v_{dc1}[V] (red line), v_{dc2}[V] (blue line).

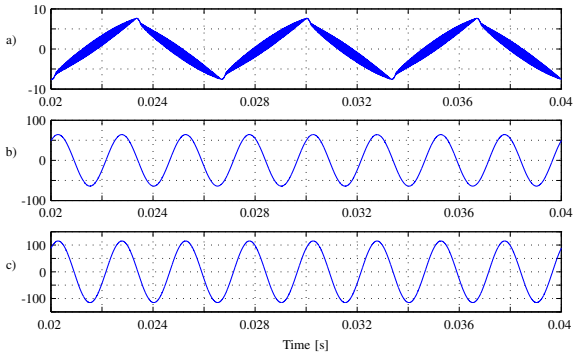

Fig. 6. GPU performance with active current injection: a) IAF current i_L[A]; b) load current i_u[A]; c) load voltage v_u[V].

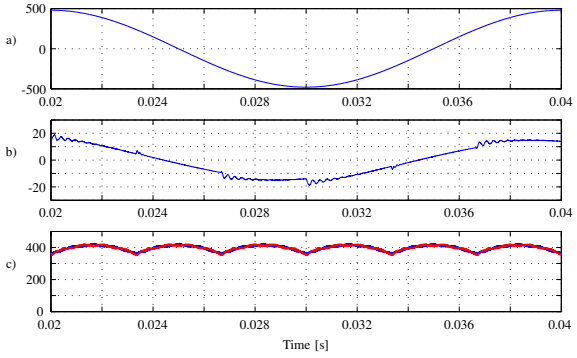

Fig. 7. Performance of the developed design: a) source voltage v_{sA}[V]; b) source current i_{sA}[A]; c) capacitor voltages v_{dc1}[V] (red line), v_{dc2}[V] (blue line).

IV. Conclusions

A new scheme of an aircraft GPU has been developed in this work. The paper describes the design of the entire unit innovating in the ac-dc and dc-ac stages. An active third harmonic injection configuration has been considered for the rectifier, while the inverter is a three-level NPC power converter. Ohmic response is attained in the mains side, while the capacitors' voltage are balanced with satisfying matching. The output voltage is is sinusoidal in accordance to the MIL-STD-704F standard.

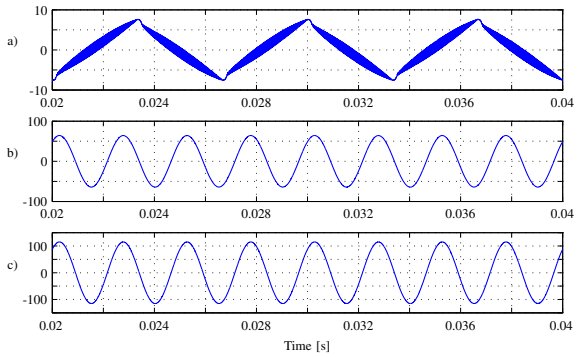

Fig. 8. Performance of the developed design: a) IAF current i_L[A]; b) load current i_u[A]; c) load voltage v_u[V].

Acknowledgment

The authors would like to thank the FONDECYT Regular 1160690 and Postdoctoral 3170014 research projects, the MEC project number 80150056 and PROCIENCIA R&D Grant 14-INV-097 for the economical support provided during the development of this research.

References

[1] S. Guenter, G. Buticchi, G. D. Carne, C. Gu, M. Liserre, H. Zhang, and C. Gerada, "Load control for the dc electrical power distribution system of the more electric aircraft," *IEEE Transactions on Power Electronics*, pp. 1–1, 2018.

[2] SAE-ARP5015A, "Ground equipment - 400 hertz gound power performance requirements," Society of Automotive Engineers, Standard, January 2011.

[3] MIL-STD-704F, "Aircraft electric power characteristics," US Department of Defense, Standard, March 2004.

[4] W. Rohouma, P. Zanchetta, P. W. Wheeler, and L. Empringham, "A four-leg matrix converter ground power unit with repetitive voltage control," *IEEE Transactions on Industrial Electronics*, vol. 62, no. 4, pp. 2032–2040, April 2015.

[5] S. L. Arevalo, P. Zanchetta, P. W. Wheeler, A. Trentin, and L. Empringham, "Control and implementation of a matrix-converter-based ac ground power-supply unit for aircraft servicing," *IEEE Transactions on Industrial Electronics*, vol. 57, no. 6, pp. 2076–2084, June 2010.

[6] M. A. Masrur, A. G. Skowronska, J. Hancock, S. W. Kolhoff, D. Z. McGrew, J. C. Vandiver, and J. Gatherer, "Military-based vehicle-to-grid and vehicle-to-vehicle microgrid-system architecture and implementation," *IEEE Transactions on Transportation Electrification*, vol. 4, no. 1, pp. 157–171, March 2018.

[7] M. Abarzadeh and K. Al-Haddad, "An improved active-neutral-point-clamped converter with new modulation method for ground power unit application," *IEEE Transactions on Industrial Electronics*, vol. 66, no. 1, pp. 203–214, Jan 2019.

[8] G. Gong, M. Heldwein, U. Drofenik, J. Minibock, K. Mino, and J. Kolar, "Comparative evaluation of three-phase high-power-factor ac-dc converter concepts for application in future more electric aircraft," *Industrial Electronics, IEEE Transactions on*, vol. 52, no. 3, pp. 727–737, 2005.

[9] M. Abarzadeh, H. M. Kojabadi, F. Deng, and Z. Chen, "Enhanced static ground power unit based on flying capacitor based h-bridge hybrid active-neutral-point-clamped converter," *IET Power Electronics*, vol. 9, no. 12, pp. 2337–2349, 2016.

[10] J. I. Leon, S. Kouro, L. G. Franquelo, J. Rodriguez, and B. Wu, "The essential role and the continuous evolution of modulation techniques for voltage-source inverters in the past, present, and future power electronics," *IEEE Transactions on Industrial Electronics*, vol. 63, no. 5, pp. 2688–2701, May 2016.

[11] U. Jensen, M. Rasmussen, T. Mortensen, F. Blaabjerg, and J. Pedersen, "A new control method for 400 hz ground power units for airplanes," in *Industry Applications Conference, 1998. Thirty-Third IAS Annual Meeting. The 1998 IEEE*, vol. 2, 1998, pp. 1469–1476 vol.2.

[12] U. Jensen, F. Blaabjerg, and J. Pedersen, "A new control method for 400-hz ground power units for airplanes," *Industry Applications, IEEE Transactions on*, vol. 36, no. 1, pp. 180–187, 2000.

[13] L. Mihalache, "Dsp control of 400 hz inverters for aircraft applications," in *Industry Applications Conference, 2002. 37th IAS Annual Meeting. Conference Record of the*, vol. 3, 2002, pp. 1564–1571 vol.3.

[14] Z. Housheng, Z. Yanlei, and L. Haidong, "Design of three-phase intermediate frequency aviation power based on single chip microcomputer," in *Computer Engineering and Technology (ICCET), 2010 2nd International Conference on*, vol. 4, 2010, pp. V4–669–V4–672.

[15] J. Zhu, Z. Nie, W. Ma, and S. Nie, "Comparison between db control and dual-loop pr control for collapsed h-bridge single-phase 400hz power supply," in *Industrial Electronics (ISIE), 2012 IEEE International Symposium on*, 2012, pp. 240–245.

[16] R. N. Beres, X. Wang, F. Blaabjerg, M. Liserre, and C. L. Bak, "Optimal design of high-order passive-damped filters for grid-connected applications," *IEEE Transactions on Power Electronics*, vol. 31, no. 3, pp. 2083–2098, March 2016.

[17] J. W. Kolar and T. Friedli, "The essence of three-phase PFC rectifier systems–part I," *IEEE Transactions on Power Electronics*, vol. 28, no. 1, pp. 176–198, Jan 2013.

[18] T. Friedli, M. Hartmann, and J. W. Kolar, "The essence of three-phase PFC rectifier systems–part II," *IEEE Transactions on Power Electronics*, vol. 29, no. 2, pp. 543–560, Feb 2014.

[19] P. Pejovic, "A novel low-harmonic three-phase rectifier," *IEEE Transactions on Circuits and Systems I: Fundamental Theory and Applications*, vol. 49, no. 7, pp. 955–965, July 2002.

[20] M. Abarzadeh and H. M. Kojabadi, "A static ground power unit based on the improved hybrid active neutral-point-clamped converter," *IEEE Transactions on Industrial Electronics*, vol. 63, no. 12, pp. 7792–7803, Dec 2016.

[21] N. Vazquez, H. Rodriguez, C. Hernandez, E. Rodriguez, and J. Arau, "Three-phase rectifier with active current injection and high efficiency," *Industrial Electronics, IEEE Transactions on*, vol. 56, no. 1, pp. 110–119, 2009.

[22] F. Donoso, A. Mora, R. Cárdenas, A. Angulo, D. Sáez, and M. Rivera, "Finite-set model-predictive control strategies for a 3l-npc inverter operating with fixed switching frequency," *IEEE Transactions on Industrial Electronics*, vol. 65, no. 5, pp. 3954–3965, May 2018.

[23] D. Boillat, T. Friedli, J. Muhlethaler, J. Kolar, and W. Hribernik, "Analysis of the design space of single-stage and two-stage lc output filters of switched-mode ac power sources," in *Power and Energy Conference at Illinois (PECI), 2012 IEEE*, Feb 2012, pp. 1–8.

[24] Y. Shanshui, L. Yan, Z. Jian, C. Mengdi, and W. Li, "Research on methods of distortion spectrum analysis for aircraft vfac power system," in *Power Electronics and Applications (EPE), 2013 15th European Conference on*, Sept 2013, pp. 1–8.

[25] R. Erickson, "Optimal single resistors damping of input filters," in *Applied Power Electronics Conference and Exposition, 1999. APEC '99. Fourteenth Annual*, vol. 2, Mar 1999, pp. 1073–1079 vol.2.